Color measurement and discrimination

Brian A. Wandell

Department of Psychology, Stanford University, Stanford, California 94305

Received September 14, 1983; accepted August 31, 1984

Theories of color-difference measurement provide a quantitative means for predicting whether two lights will be discriminable to an average observer. Consider the following color-measurement hypothesis. Suppose that two lights evoke responses from the color channels that we write as vectors, U and U′. The vector difference dU = U − U′ is itself a set of channel responses that will result from the presentation of some light. I test the hypothesis that U and U′ will be discriminable only if the light that gives rise to their differential, dU, is detectable. In the absence of a luminance component in the difference stimulus, dU, the vector-difference hypothesis holds well. In the presence of a luminance component, the theory is clearly false. When a luminance component is present, discrimination judgments depend largely on whether the lights U and U′ are in separate, categorical regions of color space.

INTRODUCTION

Color Measurement

Quantitative measurement has progressed further in color vision than in other disciplines within sensory psychology. For the simplest type of measurement, in which we attempt to decide whether two stimuli are visually equivalent, the science of color vision is a complete success. Just as methods within physics permit one to determine whether two objects—however different in shape and material—will be equivalent in weight, methods within color science permit one to determine whether two lights—however different in their spectral energy distribution—will be equivalent in appearance.

The notion of measurement includes more than the ability to identify equivalences among stimuli; we must also be able to estimate the size of differences. In sensory psychology broadly, and color science specifically, the procedure for estimating differences starts with the internal representation of the two stimuli to be discriminated. In the case of color, for example, we express each of the lights as a three-dimensional vector, say, $\mathbf{U} = (U_1, U_2, U_3)$ and $\mathbf{U}' = (U_1 + dU_1, U_2 + dU_2, U_3 + dU_3)$.

The classic approach to predicting the discriminability of two colored lights is called line-element theory (see, e.g., Ref. 1). This theory is generally stated only as a set of mathematical conditions, without detailed reference to the visual processes that give rise to the mathematical entities. Following the description of Wyszecki and Stiles,[1] we may say that line-element theory presumes that there exists a set of nine functions, $g_{ij}(\mathbf{U})$, such that the discriminability of the two lights U and U′ can be predicted by a quadratic formula

$$\sum_{i,j=1,3} g_{ij}(\mathbf{U}) d\mathbf{U}_i d\mathbf{U}_j. \quad (1)$$

[See Ref. 1, Eq. (6.7.2), p. 511.]

An important problem that arises if we limit our description to the mathematical statement—without making significant reference to the visual processes—is that it becomes operationally difficult to distinguish the effects of the prevailing illumination, which defines the observer's state of adaptation, from the effects of the test stimuli that are to be discriminated.

Consider, for example, the case of a discrimination between two test lights—presented briefly against a background—in a temporal, two-alternative, forced-choice experiment. Let us denote the background light as $\mathbf{U_B}$ and the task as the problem of discriminating $\mathbf{U_B} + \mathbf{U}$ from $\mathbf{U_B} + \mathbf{U}'$. Which term should be used as the argument to the functions g_{ij}?

In line-element theory the functions g_{ij} are introduced to describe nonlinear distortions in the color representation. A natural interpretation of these functions—closely tied to visual processes—is to assume that their value is governed by the visual process that causes most of the distortion: · light adaptation. In the context of the experiment, then, only the contribution from the background, $\mathbf{U_B}$, should be used as the argument to the line-element functions, g_{ij}. This interpretation of line-element theory supposes that nonlinearities in the representation are due entirely to the observer's state of adaptation.

This interpretation of line-element theory leads to the following expectation for color discriminations. If the observer's state of adaptation is held fixed, and the incremental test lights U and U′ are weak and briefly presented so that they do not disturb the observer's state of adaptation, then the discriminability of U and U′ can be predicted from their vector difference: (dU_1, dU_2, dU_3). In particular, we suppose that U and U′ will be discriminable if the light that would give rise to the vector difference dU = U − U′ is detectable. I will call this the vector-difference hypothesis.

The vector-difference hypothesis is a special form of line-element theory in which we tie the value of the functions g_{ij} to light adaptation. The hypothesis in its general form, however, appears in a fairly broad range of sensory measurement applications. I have reviewed the hypothesis and the difficulties that it has had in color-vision measurement elsewhere.[2] The hypothesis is also used to model discrimination of spatial and temporal patterns.[3–6]

0740-3232/85/010062-10$02.00

In this paper, I report new results showing that for test lights with slow temporal modulations, and thus little effect on the luminance system, the vector-difference hypothesis represents an adequate characterization of discrimination data. For certain experimental conditions, then, color measurement can be successfully extended to include a difference measure that predicts the discriminability of pairs of lights.

There is a substantial failure of the theory, however, when the temporal motion of the test stimuli is in a range commensurate with the flicker introduced, say, by normal eye movements. In this case, it is not possible to use the color-discrimination experiment as a basis for color-difference measurement. With flickering test stimuli containing a luminance component, the visual system abandons measurement in favor of stimulus categorization. If the luminance component is removed—by comparing only lights restricted to the isoluminance plane—the vector-difference hypothesis again provides an adequate characterization of the data.

Methods

General Considerations

The most influential analysis of color discrimination is MacAdam's work[7,8] in which the variability of color-match settings is used to estimate color discriminability. This technique and subsequent analyses[9–11] have been valuable, but they suffer from important drawbacks as well. Most significantly, the matching technique allows the subject to control the time course of the stimulus used in the discrimination judgment both by permitting the subject to adjust the intensity of the stimulus freely and by permitting the subject to view the bipartite field freely. I have chosen instead to analyze color discrimination by using a forced-choice paradigm with controlled stimulus time course. As we shall see, control of the time course is a crucial consideration.

Apparatus

The data were collected by using a specially constructed Maxwellian-view apparatus. The apparatus consists of three channels differing only in the wavelength of the light that they deliver to the observer. One channel of the apparatus is sketched in Fig. 1.

Each channel has its own lamp (quartz-halogen type). The intensity of the lamp is controlled by a closed-feedback circuit described below. The light from each bulb is first collimated and then passed through an interference filter (Baird-Atomic). The wavelengths of the filters used in all experiments reported here were 440, 540, and 650 nm.

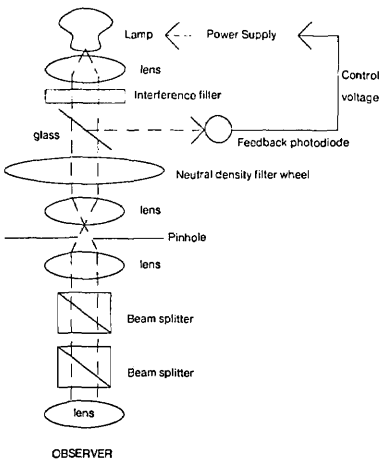

Fig. 1. Schematic diagram of one of three channels of the experimental apparatus. See text for explanation.

The narrow-band beam is split by a thin piece of glass, part of the beam falling directly on a photodiode (United Detector Technologies, pin-10) while the remainder continues to the observer. Before reaching the observer, the beam passes through one of a set of a neutral-density filters mounted on a wheel. The beam is then focused on a pinhole, recollimated, and joined together with the beams from the two other channels. The three beams are then passed through a field stop and the final Maxwellian lens.

The observer's position is held fixed at the focal point of the Maxwellian lens by means of a bite bar attached to a vise whose position is adjustable in three dimensions.

Feedback Circuitry

The fraction of light diverted from the main beam gives rise to a current from the photodiode. The current is converted to a voltage signal by an amplifier attached directly to the photodiode. This voltage provides an estimate of the amount of (monochromatic) light in the beam. This voltage is compared with a voltage provided from a digital-to-analog signal controlled by a microprocessor. Based on the difference between the desired signal level (from the microprocessor) and the actual signal (from the photodiode/amplifier), the control voltage to a voltage-programmable power supply (Hewlett-Packard Model 6282A) governing the lamp intensity is adjusted.

The intensity levels of the bulbs were varied over time by varying the voltage from the microprocessor. The design is conceptually similar to the design described by Rosen *et al.*[12] The nonlinearities in the bulb, however, make this design useful only for moderate amplitude modulations (less than 20%) and for temporal frequencies below about 12 Hz. This is adequate for detection and discrimination experiments but not so useful for studies requiring high levels of modulation for adaptation.

Stimuli

The stimuli in these experiments were all 1.85-deg spots presented upon a dark (zero) background.

Two different temporal waveforms were used for test stimuli. In one set of experiments the bulb intensities were modulated by a (roughly) Gaussian time course, with −5.0 to +5.0 standard deviations taking 1 sec. The luminance over time can be written as

$$L(t) = L_0 + C \exp\left[-\left(\frac{t-\mu}{2\sigma}\right)^2\right], \qquad t = 0, 0.01, 0.02, \ldots, 1.0, \tag{2}$$

where $\mu = 0.5$, $\sigma = 0.1$, C is the contrast, L_0 is the steady-state luminance of the background field, and t is measured in seconds. The sampling rate used to control the output is 0.01 sec, that is, 100 Hz.

In a second set of experiments, the bulb intensities were modulated by the product of the same Gaussian time course and a 6-Hz sine wave:

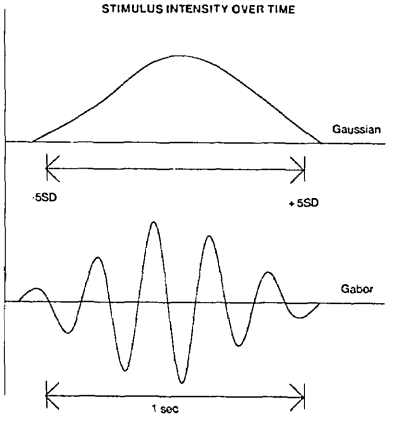

Fig. 2. Temporal waveforms of Gaussian and 6-Hz Gabor functions. The horizontal axis is time (seconds), and the vertical axis is linear intensity.

$$L(t) = L_0 + C\sin(2\pi ft)\exp\left[-\left(\frac{t-\mu}{2\sigma}\right)^2\right], \qquad t = 0.01, \ldots, 1.0. \tag{3}$$

This is commonly called a Gabor function.[13] For the experiments using a Gabor function, I used a sinusoidal frequency of $f = 6$. Figure 2 shows the intensity of the light at the observer's eye for each of these kinds of stimuli.

Calibration

Before each experimental session, we measured the amount of light at the observer's cornea. This light level could be adjusted by means of a small neutral-density wedge placed at the pinhole indicated in Fig. 1. Each channel was set to the same level, accurate to within 1.0% across sessions.

The degree of modulation caused by a control signal was measured approximately every six weeks by displaying the signals measured at the feedback circuitry using an oscilloscope with storage capabilities (Tektronix 5111). These signals permitted us to assess the linearity of the system and the gain of the apparatus. The calibration data were kept in a computer file, and the latest calibration values were (automatically) used by the programs that estimated thresholds.

Error Analysis

The response of the system is subject to two kinds of errors. The first types of errors are the nonlinearities in the circuit, the principal difficulty arising from the bulb. Measurements were restricted to amplitudes and frequencies at which nonlinearities could not be detected with the calibration equipment. The second types of errors are sampling errors introduced by the temporal sampling of the signal and the discretization of the control-signal amplitude within the range of 256 available amplitude levels.

The temporal sampling rate was kept constant at 10 msec (100 Hz). At this sampling rate, temporal aliasing below 50 Hz will not occur. (That is, the Nyquist limit for sampling at 100 Hz is 50 Hz.) Since the bulb had no measurable response to signals beyond about 30 Hz, the temporal sampling did not introduce significant distortions.

Over the varying experimental conditions it is not possible to use the full range of 256 sampling levels for every stimulus. Under some conditions, threshold-level signals may be represented by as few as five intensity levels. Of particular interest here is the degree of distortion introduced in the frequency domain at this level of intensity sampling. The relative energy spectrum of a signal with 256 levels differs by less than 1% from a signal sampled at 10 contrast levels. The contrast sampling does not introduce a significant stimulus artifact.

Detection-Threshold Estimation Procedure

Thresholds were measured by using a two-alternative, forced-choice, multiple-staircase design. The initial stimulus level was set by hand to a contrast level at which the stimuli were judged barely, but regularly, detectable. Starting near this level, four independent staircases were run in each block, each staircase continuing for 25 trials. The staircase rule was as follows: After each incorrect response, increase the contrast of the signal by 2 dB; after two correct responses, decrease the contrast of the signal by 2 dB.

Threshold estimates are generally based on two or three sessions, for a total of 200–300 observations per data point. A single psychometric function was fitted to the data pooled across sessions. The Weibull (see Ref. 14) was used for its convenience and theoretical significance[15]:

$$P(\text{cor}) = \frac{1}{2} + \frac{1}{2}\exp\left[-\left(\frac{C}{\alpha}\right)^{\beta}\right], \tag{4}$$

where C is the stimulus contrast. At the contrast level α, the observer is correct on 81% of the trials, and this value is plotted as threshold.

The data were fitted to the Weibull by using a maximum-likelihood procedure described by Watson.[16] The fitting procedure has been analyzed by Maloney and Wandell,[17] who used a bootstrap simulation method. Maloney and I found that estimates of the intensity level at which 81% probability correct is obtained are stable (plus or minus one standard error) to within about 5% (linear intensity) when the fitting procedure based on 200 forced-choice observations is used. Further, for the stimuli used in this study, the value of the parameter β is generally near 2. This value is significantly lower than the value commonly found for grating detection (cf. Ref. 18) and quite close to the value commonly found for Stiles's increment-threshold procedure[19] (cf. Refs. 15 and 20).

Discrimination-Threshold Estimation Procedures

In the discrimination measurements, the observer is presented with a weak pedestal light, Π, and a pedestal light plus an increment, $\Pi + \Delta$. In the experiments reported here, the pedestal and the increment always had the same time course. The observer must identify which of the intervals contained the pedestal plus the increment.

In these experiments only the contrast of the increment Δ is varied. The same staircase rule is followed as in the detection procedure. Two correct discriminations lead to a reduction in the contrast of the increment; any error leads to an increase in the increment. The detection-threshold experiment may be viewed as the special case of the discrimination experiment in which the pedestal light, Π, is zero.

DETECTION

Representation

Results are plotted using a linear coordinate system. Each axis represents the linear intensity of a primary light. In Fig. 3, the intensity of the 650-nm channel at threshold is plotted on the horizontal axis and the intensity of the 540-nm channel is plotted on the vertical axis. The origin of the graph is at the steady level. The steady level establishes the state of adaptation. The absolute quantal levels and the chromaticity of the adapting lights are indicated in the figure caption.

The modulations of the test lights at threshold are plotted on the graph at the contrast of the stimulus during its presentation. The contrast of the stimulus is computed as follows: Let the value of the intensity at its largest deviation from steady be I_p, and let the steady-state intensity be I_0. Then the stimulus contrast is

$$(I_p - I_0)/I_0. \tag{5}$$

Symmetry of Gabor Functions

When the 6-Hz Gabor function is used, a shift from positive to negative contrast is equivalent to a shift of 180 deg in the sinusoidal term. Such a shift is of no visual significance, so that the detectability of a 6-Hz Gabor function with both contrast terms positive (plotted in the upper-right-hand quadrant of Fig. 3) will always be the same as the detectability of a 6-Hz Gabor function with both contrasts negative (plotted in the lower-left-hand quadrant). This forces a symmetry on the 6-Hz Gabor data that is not present in the Gaussian data. I took advantage of this symmetry and made measurements only between 0 and 180 deg (measuring counterclockwise from the x axis) for 6-Hz Gabor stimuli. The detection data points are plotted twice, however, for easier comparison with the Gaussian threshold measurements.

Gaussian Perturbations

With these conventions, Fig. 3 represents the detection contour of a Gaussian perturbation of the adapting field. The adapting field in this condition was metameric to a 630-nm light.

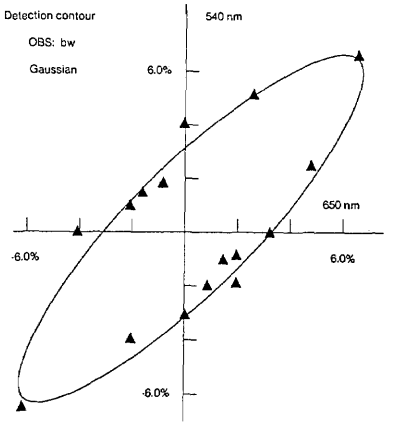

Fig. 3. Gaussian detection contour for observer bw. The mean adapting level (origin of the graph) is a mixture of 650-nm light at 9.93 log quanta deg^{-2} sec^{-1} and 540-nm light at 8.52 log quanta deg^{-2} sec^{-1}. The chromaticity coordinates of the adapting point are (0.703, 0.296, 0.001) approximately equivalent to 630 nm. The axes measure the percent contrast of each component of the signal. The smooth curve sketches the maximum-likelihood isodetection contour at 81% correct estimated from the model described later in the text.

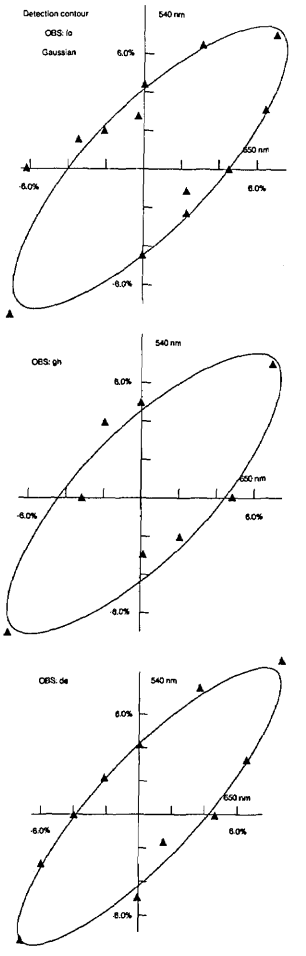

Fig. 4. The three panels represent Gaussian data from three more observers. The conditions are the same as for Fig. 3.

Test Inhibition

Two properties of the detection contour are striking. First, consider the upper-right-hand quadrant. In this quadrant, the experiment consists of measurement of test additivity between two positive Gaussians (luminance increment). There is a clear inhibition between 540- and 650-nm modulations: Admixing 650-nm test light with 540-nm test light makes the 650-nm test light less visible.

In the lower-left-hand quadrant, we measure mixtures of pairs of decrements (luminance decrement). Again the data show that over a significant range there is a strong inhibition between the 650- and 540-nm decrements.

This inhibition is among the strongest reported in the literature (cf. Ref. 21).

Mechanism Linearity

A second significant property is that, when the Gaussian time course is used, the detection contour is quite elongated. The data may be viewed either as falling along an extremely eccentric ellipse or as having two sides that are roughly linear. Either interpretation is consistent with the hypothesis that the underlying mechanisms are linear near threshold. The linearity will be revealed, however, only when one of the

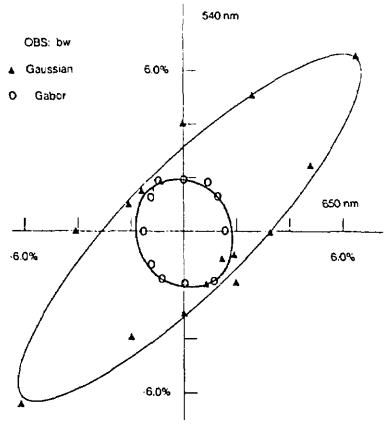

Fig. 5. Sensitivity to a 6-Hz Gabor test stimulus (open circles) compared with the data in Fig. 3 (filled triangles). Adapting conditions are as in Fig. 3.

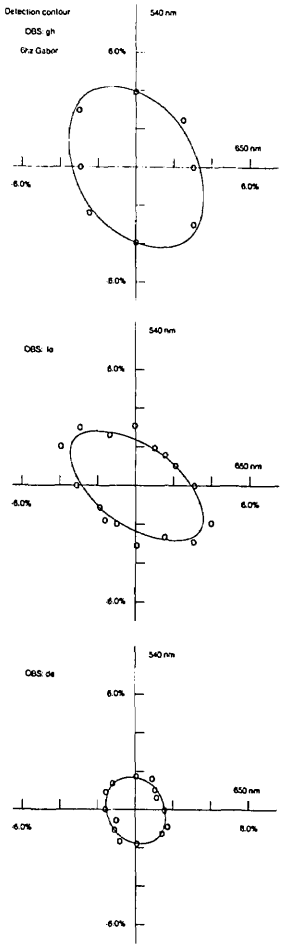

Fig. 6. The three panels plot data for several observers using a 6-Hz Gabor function. Adapting conditions are as in Fig. 3.

mechanisms has generally much greater sensitivity than all others, thereby exposing itself over a larger region of the threshold contour.

If the underlying detection mechanisms are linear, we also expect that the data will fall symmetrically about the origin, as they do. The linearity of the sides and the symmetry about the origin are replicated in the detection contours of all the observers whom we have tested. Data from several observers are shown in Fig. 4. The detection contours of the various observers measured in this experiment are in quite close quantitative agreement.

6-Hz Gabor Perturbations

In Fig. 5, I have plotted the detection contour of the 6-Hz Gabor time course and the detection contour of the Gaussian time course on a common axis.

Test Additivity

Unlike the Gaussian data, the mixture of 6-Hz 540- and 650-nm lights does not inhibit visibility. The 6-Hz Gabor detection contour is considerably less elliptical, having none of the extended contours as in the Gaussian data. The increased circularity in all the observers' data is replicated in Fig. 6.

A common working hypothesis[22–24] is that the absence of test inhibition and change in sensitivity in the 45-deg direction occurs because of a luminance channel that is sensitive to flicker in the 45–225-deg directions but insensitive to the Gaussian perturbation. The 6-Hz Gabor data reveal the luminance mechanism and conceal the linear threshold contour of the opponent mechanism.[25]

INTERMEDIATE DISCUSSION

Color-Difference Measurement

I now turn to the problem of color measurement and color discrimination. The question that I pose is the following: To what extent can we predict the discriminability of pairs of lights not greatly different in intensity from the adapting field? The question is posed graphically in Fig. 7.

The simplest answer to this question, offered by the vector-difference hypothesis, is that **U** will be *discriminable* from **U′** when the differential response between them, $d\mathbf{U} = \mathbf{U} - \mathbf{U}'$, is equivalent to the response caused by a light that is *detectable*.

Since the detection contour defines the contrast of the physical stimulus required for a just-detectable perturbation of the visual mechanisms, according to theory we should be

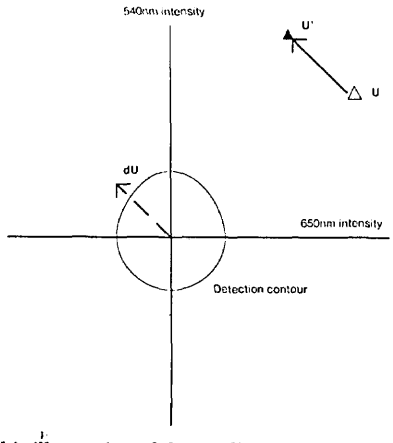

Fig. 7. Graphic illustration of the predictions of the vector-difference hypothesis concerning the discriminability of two points, labeled **U** and **U′**, that are small perturbations of the adapting field. The two points are predicted to be different if the vector difference between them (solid vector), when displaced to the origin (dashed vector), extends beyond the detection contour.

able to predict the discriminability of lights by determining whether the difference vector dU falls inside or outside this contour.

The vector-difference hypothesis is independent (up to an arbitrary, invertible, linear transformation) of the coordinate system in which the stimuli are represented. To see this, suppose that dU represents a detectable light in one coordinate system, so that in this coordinate frame two lights with a vector difference $\mathbf{U} - \mathbf{U}' = d\mathbf{U}$ will be discriminable. If we represent the lights in a new coordinate system, differing by a linear transformation T, then $T d\mathbf{U}$ is the same light, so it is detectable. The new representations for U and U′ are $T\mathbf{U}$ and $T\mathbf{U}'$, and their vector difference is $T\mathbf{U} - T\mathbf{U}' = T(\mathbf{U} - \mathbf{U}') = T d\mathbf{U}$, so they again will be predicted to be discriminable.

DISCRIMINATION

Representation

The discrimination thresholds are plotted as pairs of points following the same conventions and using the same axes as the detection thresholds. One of the points (plotted as an open symbol) represents the pedestal, Π, and the second point (plotted as a filled symbol) represents the pedestal plus the increment, $\Pi + \Delta$, at which discrimination occurs at the 0.81 probability correct level. The vector difference between the two lights represents the increment alone, Δ. By the vector-difference hypothesis, the length of the difference vector must be constant, independent of the pedestal (when the pedestal is a weak perturbation of the adapting field) and equal to the length of the vector at detection threshold.

Gaussian Perturbations

One set of discrimination thresholds, for a Gaussian test stimulus, is plotted in Fig. 8. The pedestal points (open symbols) fall along a straight line at a 22.5-deg angle to the x axis. These points fall on a perfectly straight line because they are chosen by the experimenter. With each pedestal point, there is an associated pedestal plus increment (filled symbols), separated from the pedestal by a difference vector oriented 135 deg (counterclockwise) relative to the x axis. The points defining the pedestal plus the difference fall closely parallel to the line of points defining the pedestal, indicating that the size of the difference vector is approximately constant and is independent of the pedestal. Under these stimulus conditions, the vector-difference hypothesis is satisfied.

Figure 9 plots further tests of the vector-difference hypothesis using the Gaussian perturbations of the field. The pedestals fall along straight lines on the x axis and 45 deg below the x axis. In all measurements, the test vector is oriented at 135 deg to the x axis. The pedestal lines and the associated pedestal-plus-increment lines are approximately parallel, as required by the vector-difference hypothesis.

For the 13 discrimination measurements in Figs. 8 and 9, the mean value of the difference vector is a contrast of 2.54% with a standard deviation of 0.3% (standard error of the mean, 0.09%). Of the 13 measurements only one point lies more than two standard deviations (SD's) from the mean (−2.17 SD). These measurements do not permit us to reject the hypothesis.

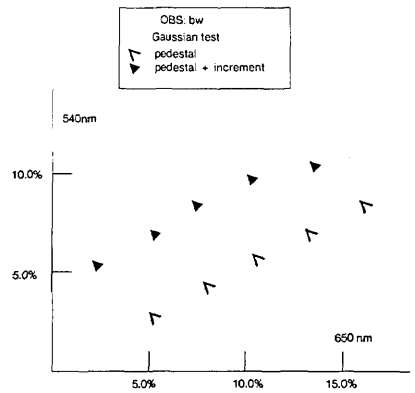

Fig. 8. Pairs of points at discrimination threshold. One point in each pair, the pedestal, is plotted as an open symbol. This point is fixed by the experimenter. The position of the second light, the pedestal plus the increment, is plotted as a filled symbol. This point may fall anywhere along a line at 135 deg (counterclockwise) to the horizontal axis, starting at the pedestal. The pedestal points were chosen to fall along a line oriented at 22.5 deg counterclockwise to the horizontal axis. The pedestal contrasts extend over a range up to roughly 2.5 times threshold. Adapting conditions are as in Fig. 3.

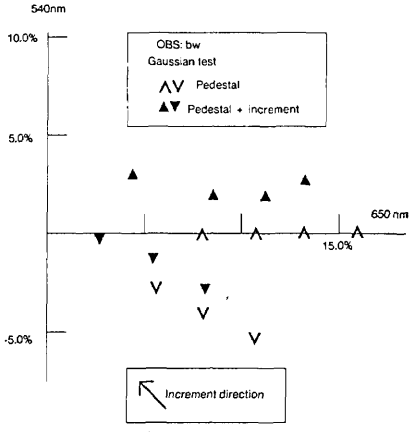

Fig. 9. Additional discrimination thresholds, following the conventions in Fig. 8. The new pedestal directions are at 0 deg (along the horizontal axis) and 45 deg below the horizontal axis. Adapting conditions are as in Fig. 3.

A Further Test

In Fig. 10, I plot a further test of the hypothesis. In the previous test, the pedestal was varied for each discrimination threshold, and the increment was constant. In this test, the pedestal is constant, and the direction of the increment is varied. By sweeping out the discrimination thresholds for different directions of the increment, we create discrimination contours in analogy to the detection contour (the special case in which the pedestal light is zero). We expect, on the vector-difference hypothesis, that the discrimination contours will have the same geometric shape as the detection contours.

In the top portion of Fig. 10, I plot the detection contour along with the discrimination contours represented around their respective pedestal lights. The bottom portion of the figure represents the same data but with the discrimination contours slid so that the pedestal lights are at the origin. This is done to facilitate comparison of the different shapes. Figure 11 displays a replication of these data on a second observer.

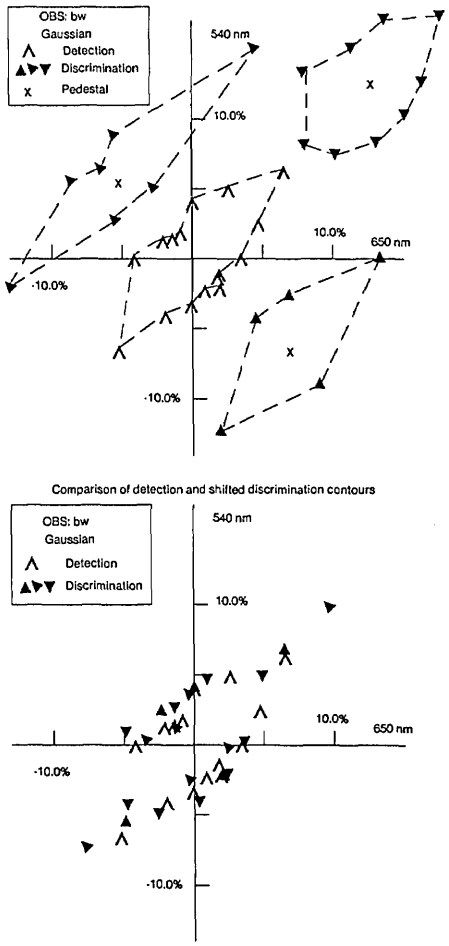

Fig. 10. Detection contour (open symbols) and several discrimination contours (filled symbols) for Gaussian test stimulus. In the top panel, the discrimination thresholds for various directions around the pedestal are plotted around the position of their respective pedestals (indicated by an ×). In the bottom panel, to permit comparison of the shapes of the discrimination contours, the data have been slid so that the pedestals fall at the origin. Adapting conditions are as in Fig. 3.

Under these conditions, the data are generally consistent with the vector-difference hypothesis. Although there may be some small, measurable differences (particularly for test lights in the 45-deg direction), the hypothesis serves as an excellent first-order approximation to the large potential set of discrimination judgments.

I have already shown, however,[2] that the vector-difference hypothesis does not hold under all measurement conditions. In the next section, I show that the time course of the lights is crucial in determining whether the hypothesis can successfully describe the data.

Discriminations with a 6-Hz Gabor Function

In Fig. 12, I plot discrimination thresholds using the 6-Hz Gabor functions. As in the Gaussian data, pedestal positions fall along straight lines: In the top panel, the angle is 22.5 deg; in the middle panel, it is 45 deg; and in the bottom panel, it is 67.5 deg. In all three panels, the increment was in the 135-deg direction.

Categorization of Stimulus Regions

Figure 12 demonstrates a clear failure of the vector-difference hypothesis. In the top panel, the length of the difference vector separating the pedestal and the pedestal plus the increment increases with the contrast of the pedestal. This trend is slightly evident in the middle panel and not evident in the lower panel. The failure is quite regular and predictable.

In Fig. 13, I have plotted all the pedestal-plus-increment data points from Fig. 12. These points fall approximately along a common line in stimulus coordinate space, despite the fact that the pedestals from which they are being discriminated fall across a fairly wide range of stimulus space. This plot reveals that the contrast of the incremental term is not critical when predicting whether two lights will be discriminable. For example, discrimination thresholds measured from the 22.5-deg line can be as much as 2.5 times greater than the discriminations made along the same line but measured starting from the 67.5-deg direction. The key factor in determining discriminability appears to be whether the two lights fall in a common region or in separate regions of color space. *It is the visual system that defines where this border falls.*

The same type of deviation can be seen for a second observer, who used a 6-Hz Gabor function but a different adapting point, pedestal, and test directions. These are plotted in Fig. 14. The common border is illustrated in Fig.

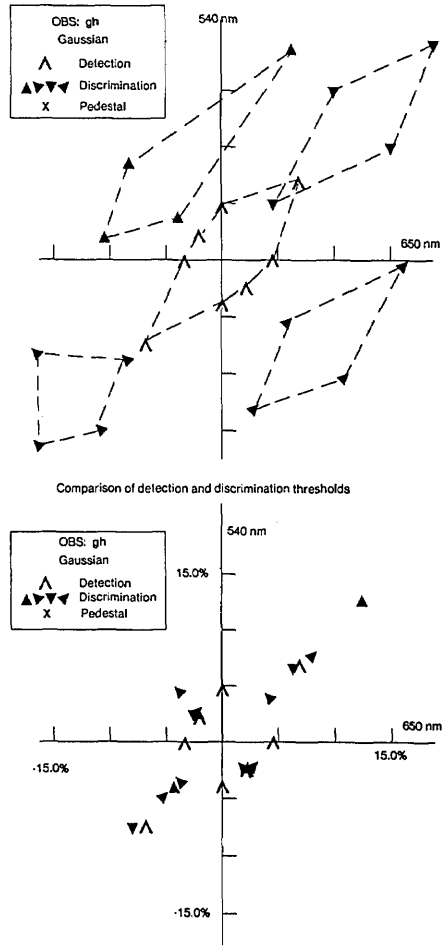

Fig. 11. As in Fig. 10 but for a second observer.

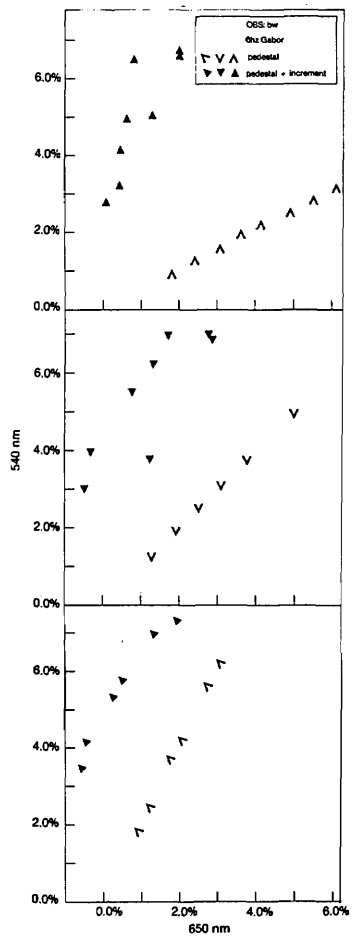

Fig. 12. Pairs of points at discrimination threshold, using a 6-Hz Gabor function. The plotting conventions are as in Fig. 8. Each panel represents a pedestal at a different direction. Panels: top, 22.5 deg; center, 45 deg; bottom, 67.5 deg. Adapting conditions as in Fig. 3.

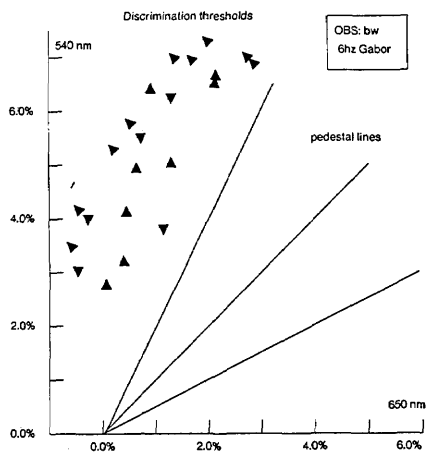

Fig. 13. The filled symbols replot all the pedestal-plus-increment data points from Fig. 12. The lines indicate the range of values of the pedestals in that figure. The pedestal-plus increments fall roughly along a common line despite the wide range of angles swept out by the pedestals. Adapting conditions as in Fig. 3.

15. I have replicated this pattern of discrimination results under various adapting conditions with various combinations of pedestal and increment.

The failure of the vector-difference hypothesis occurs for lights that are at detection threshold. It is unlikely that the failure of the vector-difference hypothesis is due simply to a loss of sensitivity caused by the pedestal. For measurements in some pedestal directions there is no loss of sensitivity with pedestal contrast. This is illustrated in Fig. 16, which is a set of discrimination thresholds in various directions around a pedestal in the 22.5-deg direction.

In Fig. 16, a detection contour and discriminations around a pedestal position at 22.5 deg are plotted. The pattern of discriminations is quite different from the pattern of detections, again indicating a failure of the vector-difference hy-

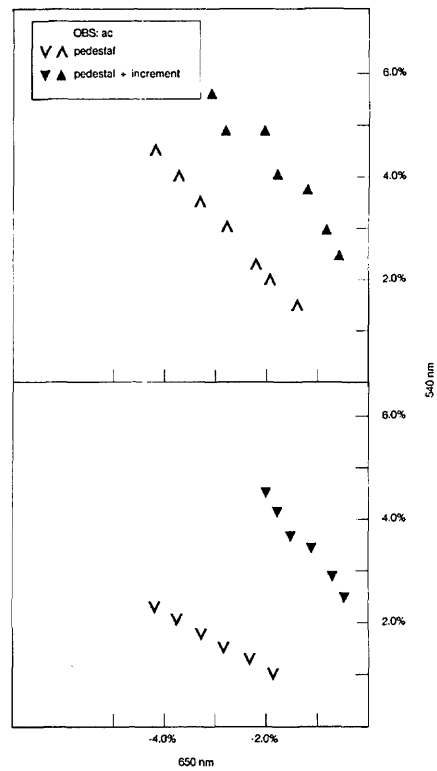

Fig. 14. Discrimination thresholds for pedestals falling along the 135-deg direction and the incremental vector in the 45-deg direction. The adapting conditions for these data were similar to those for the previous data (see Fig. 3), except that a steady blue field at 8.381 log quanta deg^{-2} sec^{-1} was added to the steady background. The chromaticity coordinates of the adapting field are off the spectral locus at (0.683, 0.285, 0.032). The observer is ac.

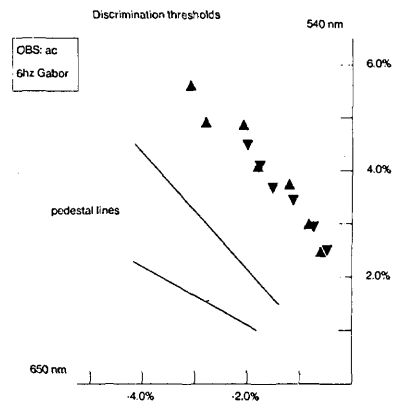

Fig. 15. A replot of the pedestal plus test data points from Fig. 14. The points fall along a common line.

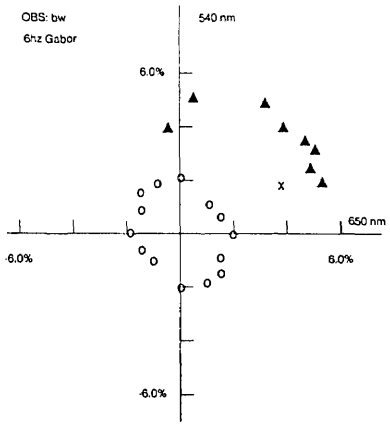

Fig. 16. Discrimination thresholds for different directions around a pedestal in the 22.5-deg direction. Adapting field as in Fig. 14. Notice that the shapes of the contours are quite different and that discriminations in the direction away from the pedestal vector strongly violate the vector-difference hypothesis. Observer is bw.

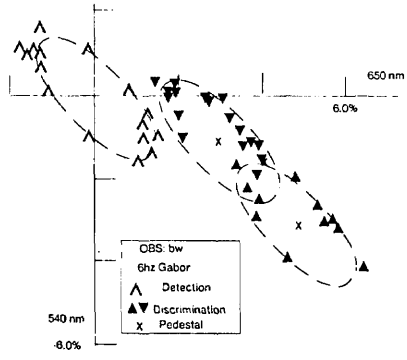

Fig. 17. Detection contour (open symbols) and discrimination contours (filled symbols) of 6-Hz Gabor functions modulated in the isoluminance plane. The adapting field is described in Fig. 14. Stimulus coordinates for two of the channels are plotted, and the modulation of the third beam (440 nm) can be determined from the other two since the combination of modulations must remain within the isoluminance plane. Although three discrimination contours were measured, only two are shown in this figure in order to avoid cluttering the graph. The third is presented in Fig. 18. Observer is bw.

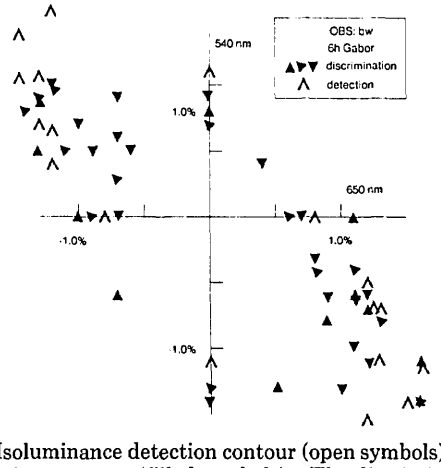

Fig. 18. Isoluminance detection contour (open symbols) and three discrimination contours (filled symbols). The discrimination contours have been slid so that their pedestals fall on the origin to permit a comparison of the shapes of the discrimination contours and the detection contour. Adapting conditions are as in Fig. 14. Observer is bw.

pothesis. The failure is such that test sensitivity in the 135-deg direction is decreased, while sensitivity in the 315-deg direction is essentially unchanged. The pattern of results is consistent with the idea that discrimination of increments away from the principal direction of the pedestal shows categorical performance limits.

Nature of the Visual Mechanisms

There can be no doubt that there is a dramatic shift in discrimination behavior as the time course of the stimulus is varied. In analyzing the detection data I argued that differences in the properties of the detection contour occur because detection is mediated by visual mechanisms that are different when the Gaussian time course is used from those when the 6-Hz Gabor time course is used. This may also be the reason for the shift in discrimination performance. In particular, if the 6-Hz Gabor function is a potent stimulus for a luminance mechanism, the shift in discrimination behavior may be due to a role played by the luminance channel.

To test this hypothesis, I have measured the discriminability of 6-Hz Gabor functions modulated entirely within the isoluminance plane. Measured in this way, discrimination behavior among 6-Hz Gabor functions cannot depend on the response of the luminance mechanism. The detection and discrimination contours for such isoluminance data are plotted in Fig. 17. The coordinate system used in this plot is also a stimulus-based coordinate system, as in the previous plots. The degree of contrast modulation for two of the test stimulus channels are plotted explicitly as the horizontal and vertical axes. The contrast of the third test channel may be inferred from the contrast of the other two, as this contrast is determined by the fact that the total stimulus must be kept in the isoluminance plane.

In Fig. 18, I plot the detection and discrimination contours slide so that the pedestals fall on the origin. The agreement in shape here is about as good as the agreement found when the Gaussian stimulus is used, and it is far better than the agreement found when the 6-Hz Gabor is allowed to vary in luminance. The 6-Hz Gabor data measured with no luminance component are consistent with the vector-difference hypothesis. These data support the view that categorization of discrimination responses occurs because of a role played by a luminance mechanism.

CONCLUSIONS

When discrimination depends principally on opponent-channel responses, discrimination thresholds can be predicted from the detection contour alone. This observation is consistent with a classic view of color measurement of small color differences described by the vector-difference hypothesis.

When the luminance mechanism is differentially excited by the test lights, discrimination judgments have a categorical quality. It is not simply the size of the differential response among visual mechanisms that determines if two lights will be discriminable but rather whether the differential responses fall on different sides of a boundary set by the visual system in color space. This observation is not consistent with a classic view of color measurement of small color differences described by the vector-difference hypothesis.

The vector-difference hypothesis asserts that there is a smallest-detectable perturbation and that all detection and

discrimination judgments work at this resolution limit. Categorical responses, however, represent a different type of limit on discriminability. Differences that exceed this resolution limit are ignored if they do not cross a boundary imposed by visual processing. Two reasons for adopting this processing method are the following.

First, categorical limits may provide a means of focusing visual processing on those channels where dynamic stimulus events are clearly signaled. If estimating the perturbation of a channel containing a clear signal may take precedence over monitoring weaker perturbations in a second channel, then using a categorical limit reduces processing of the secondary channel, since no variations in the secondary channel will be attended to until the response exceeds some fixed value. If this hypothesis is true, the results here suggest that automatic allocation of attention may occur between luminance and chromatic channels but not between chromatic channels.

Second, the estimation of spectral properties of surfaces must depend on some assumptions concerning the distribution of surface boundaries and ambient-lighting conditions. Comparison of colors against different backgrounds or under spatially and temporally varying lighting conditions cannot proceed with the same fine-grained level of measurement as under conditions in which the background surface and lighting are constant. If luminance signals are used to indicate whether the physical environment meets the assumptions required for accurate visual estimation of spectral information, then the method of assessing color differences will shift when luminance components are introduced into the test stimuli.

ACKNOWLEDGMENTS

This research was supported by grant no. 2 RO1 EY03164 from the National Eye Institute, contract F33615-82-K-5108 from the U.S. Air Force, and grant no. NASA-NCC-2-44 from the National Aeronautics and Space Administration. I thank J. Farrell, W. Cowan, D. Krantz, G. Loftus, L. Maloney, and E. Markman for their comments on the manuscript.

REFERENCES

1. G. Wyszecki, and W. S. Stiles, *Color Science* (Wiley, New York, 1967).
2. B. A. Wandell, "Measurements of small color differences," Psychol. Rev. **89,** 281–302 (1982).
3. F. W. Campbell and J. G. Robson, "Application of Fourier analysis to the visibility of gratings," J. Physiol. (London) **197,** 551–566 (1968).
4. D. Sagi and S. Hochstein, "Discriminability of suprathreshold compound spatial frequency gratings," Vision Res. **23,** 1595–1608 (1983).
5. A. B. Watson, "Detection and recognition of simple spatial forms," NASA Tech. Memo. 84353.
6. H. R. Wilson and D. J. Gelb, "Modified line-element theory for spatial-frequency and width discrimination," J. Opt. Soc. Am. A **1,** 124–131 (1984).
7. D. L. MacAdam, "Visual sensitivities to color differences in daylight," J. Opt. Soc. Am. **32,** 247–274 (1942).
8. D. L. MacAdam, "Specification of small chromaticity differences," J. Opt. Soc. Am. **33,** 18–26 (1943).
9. L. Silberstein and D. L. MacAdam, "The distribution of color matchings around a color center," J. Opt. Soc. Am. **35,** 32–39 (1945).
10. W. R. J. Brown, "The influence of luminance level on visual sensitivity to color differences," J. Opt. Soc. Am. **41,** 684–688 (1951).
11. W. R. J. Brown, "Statistics of color-matching data," J. Opt. Soc. Am. **42,** 252–256 (1952).
12. P. Rosen, M. W. Levine, M. Rosetto, and I. Abramov, "A system for controlling the light output of a monochromator by any simple function and for temporally modulating intensity," Behav. Res. Methods Instrum. **2,** 297–300 (1970).
13. D. Gabor, "Theory of communication," J. IEE (London) **93,** 429–457 (1946).
14. R. F. Quick, "A vector magnitude model of contrast detection," Kybernetik **16,** 65–67 (1974).
15. L. T. Maloney and B. A. Wandell, "A model of a single visual channel's response to weak test lights," Vision Res. **24,** 633–640 (1984).
16. A. B. Watson, "Probability summation over time," Vision Res. **19,** 515–522 (1979).
17. L. T. Maloney and B. A. Wandell, "The slope of the psychometric functions at different wavelengths," Invest. Ophthalmol. Visual Sci. Suppl. **24,** 183A (1983).
18. J. Nachmias, "On the psychometric function for contrast detection," Vision Res. **21,** 215–223 (1981).
19. W. S. Stiles, "Mechanism concepts in colour theory," J. Colour Group **11,** 106–123 (1967).
20. B. A. Wandell, P. Ahumada, and D. K. Welsh, "Reaction times to weak test lights," Vision Res. **24,** 647–652 (1984).
21. J. Thornton and E. N. Pugh, Jr., "Red/green color opponency at detection threshold," Science **219,** 191–193 (1983).
22. D. H. Kelly and D. van Norren, "Two-band model of heterochromatic flicker," J. Opt. Soc. Am. **67,** 1081–1091 (1977).
23. S. L. Guth, N. J. Donley, and R. T. Marrocco, "On luminance additivity and related topics," Vision Res. **9,** 537–575 (1969).
24. B. A. Wandell and E. N. Pugh, "Detection of long-duration, long-wavelength incremental flashes by a chromatically coded pathway," Vision Res. **20,** 625–636 (1980).
25. A clear example expressing the view that flickering lights cause a luminance response may be found in Ref. 23, p. 568:

    We have long theorized that judgments made in a flicker photometric situation are mediated by the non-opponent system. This is almost self-evident, since flicker photometry demands that judgments of minimum flicker be made after chromatic fusion has occurred. That is, the procedure is presumably dependent upon the fact that the non-opponent system is temporally more sensitive than the chromatic system.